

# Quasar 3C273

## Optical Spectrum and Determination of the Redshift

Recorded with the DADOS Spectrograph  
and the CCD Camera Atik 314L +

Richard Walker, CH-Rifferswil

[richiwalker@bluewin.ch](mailto:richiwalker@bluewin.ch)

Version 1.2    July 2013



## Table of Contents

<b>1</b>	<b>Introduction .....</b>	<b>4</b>
<b>2</b>	<b>Quasar 3C273 .....</b>	<b>4</b>
<b>3</b>	<b>Key Data of 3C273 .....</b>	<b>4</b>
<b>4</b>	<b>Identification and Properties of the Spectral Lines .....</b>	<b>5</b>
<b>5</b>	<b>The Redshift of the Spectral Profile.....</b>	<b>7</b>
<b>6</b>	<b>Estimation of the Apparent Recession Velocity .....</b>	<b>9</b>
<b>7</b>	<b>Estimation of the Distance .....</b>	<b>9</b>
<b>8</b>	<b>Variations in the Spectral Profile .....</b>	<b>10</b>
<b>9</b>	<b>Relative Radiometric Flux Correction of the Profile.....</b>	<b>10</b>
<b>10</b>	<b>Recording of the Spectrum – Considerations and Details.....</b>	<b>13</b>
<b>11</b>	<b>Bibliography and Internet Links .....</b>	<b>15</b>

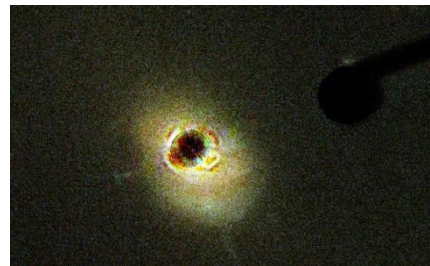
## 1 Introduction

The apparently brightest Quasar 3C273 in Virgo is often (wrongly) called the most distant object which can still be seen with average amateur means, purely visually and without the use of astro cameras. This document sets out which information can be obtained - using a low-resolution slit spectrograph, enabling relatively short exposure times, and a cooled astronomical CCD camera of the latest generation.

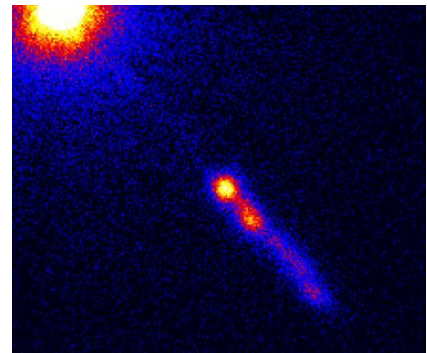
## 2 Quasar 3C273

The designation means the object number 273 in Ryle's third Cambridge catalogue of radio sources from 1959. The term "Quasar" is derived from *Quasistellar Object (QSO)*, because these objects appear as point shaped light sources. Maarten Schmidt discovered the first in 1963 at the coordinates of a corresponding entry in the mentioned radio source catalogue. It quickly became clear that this object showed the largest Redshift, known at that time, and therefore could impossibly be a star. In addition, the obtained spectra differed dramatically from stellar profiles and appeared more like those of Wolf Rayet stars, Nova outbursts, or even Supernova explosions.

According to today's knowledge, Quasars are considered as the most energetic and luminous version of active galaxies. The center of such an object always hosts a supermassive Black Hole which accumulates matter from the surrounding galaxy by an accretion disk. Therefore, Quasars are also strong sources of X-ray and radio emission. Their point shaped appearance can be explained by the enormous brightness of the nuclei, which in most cases totally outshine the rest of their host galaxies (HST image: 3C273). Apart from the episodically occurring Supernova explosions they are by far the most luminous objects in the universe.



The image of the X-ray satellite CHANDRA (source Wikipedia) shows a jet with a length of estimated 200,000 ly. It is generated by a part of the accretion flow, which is deflected in the direction of the Black Hole's rotation axis. Because Quasars are observed at very large distances only, we may see here an early stage of the galactic evolution. Even ordinary galaxies like the Milky Way host massive Black Holes in their central "bulge", which ceased the accretion process since a long time.



## 3 Key Data of 3C273

According to [1], [2], [5], [6]:

- Coordinates (epoch J2000): 12h 29' 06.7" +02° 03' 09"
- Redshift  $z \approx 0.1583$
- Expansion of the space-time lattice ("escape velocity"):  $c \cdot z \approx 47'469.1 \text{ km s}^{-1}$
- Apparent magnitude (slightly variable)  $V \approx +12.7^m$
- Absolute magnitude:  $-26.7^m$

The mass estimation of the Black Hole is still difficult and uncertain. The literature shows strongly scattering values for example [6], proposing a mass of some 1 bn  $M_{\odot}$ .

## 4 Identification and Properties of the Spectral Lines

Despite the extreme Redshift of the spectrum, in this sect. 4 and in the following table, the spectral lines are discussed and displayed with their rest wavelengths  $\lambda_0$ . The Redshift and its consequences are discussed later in sect. 5. The redshifted original scale was calibrated with a modified OSRAM glowstarter bulb, containing Argon- and Hydrogen gas [25]. The scale of the *rest wavelength* was calibrated directly with the known  $\lambda_0$  values of the H-Balmer series.

The identification of the spectral lines is chiefly based on [4], [5], [6], [7], [8]. The spectrum is dominated by extremely broadened emissions of the H-Balmer series and by forbidden [OIII] lines at  $\lambda\lambda$  5007 and 4959, fusing here to a blend. Because of quantum mechanical reasons, the forbidden lines can not appear significantly broadened, it is discussed whether the  $\lambda$  5018 emission of the Fe II (42) multiplet ( $\lambda\lambda$  4923, 5018 and 5169) supplies the major contribution to the intensity of this emissions [4], [7]. This multiplet frequently appears in the spectra of Active Galactic Nuclei (AGN), as well as in the profiles of Protostars (see [21], sect. 13). Striking is the much lower intensity of the O III emission, relative to H $\beta$ . This observation is in contrast to the spectral profiles of active Seyfert-type Galaxies, planetary nebulae and H II regions (see [21], sect. 24). This phenomenon has already been noted by the discoverers of Quasars in the 1960ies. Even today just hypotheses exist about this issue.

Undisputed is the Ne III emission at  $\lambda$  3869. The other features are mostly broad-band blends of different emissions, generated by various ions. This significantly complicates the line identification [7]. Consequently, their exact composition is still unclear. Striking is a broad emission between  $\lambda\lambda$  4500-4700. *J. B. Oke* [8] suggested as the cause the He II line at  $\lambda$  4686 and numerous emissions of C III and N III - this in analogy with similar spectra of Supernovae and Wolf Rayet stars.

In [7] it is assumed that the striking emission in the range of  $\lambda$  5870 is caused by He I at  $\lambda$  5876. Under discussion is also the Na I doublet, which in certain phases can be observed during Nova eruptions. Due to the extreme shock sensitivity of the metastable initial states of the forbidden O III lines, and the very low ionisation energy of Na I, these emissions must necessarily be generated at a considerable distance to the supermassive Black Hole. An indication for the contraction process within the accretion disk are the inverse P Cygni profiles in the area around  $\lambda\lambda$  6100 - 6400, also observable in the spectra of the much smaller disks around the T Tauri and Ae/Be- Protostars (see [21], sect. 13). The H $\alpha$  emission is redshifted so far that it coincides with the intense, telluric Fraunhofer A line. This is the cause why H $\alpha$  appears split here [8]. This circumstance complicates the determination of the Redshift, using this line (see sect. 5), and seems at least to be one of the reasons for the by far too low Balmer Decrement ( $I_{H\alpha}/I_{H\beta} < 2.85$ ) [8]. Therefore, the radial velocity in the vicinity of the Black Hole is estimated here, using the FWHM of the Doppler-broadened and Gauss fitted H $\beta$  line. Infos to the formula see [20], sect. 17. At such extreme line widths the correction of the instrumental broadening is not necessary.

$$FWHM_{Emission\ H\beta} \approx 88\text{\AA}$$

The radial velocity of the matter, calculated with the Doppler principle results in:

$$v_r \approx \frac{FWHM_{Emission\ H\beta}}{\lambda_{0\ H\beta}} \cdot c \approx 5400\ km/s \quad \{1\}$$

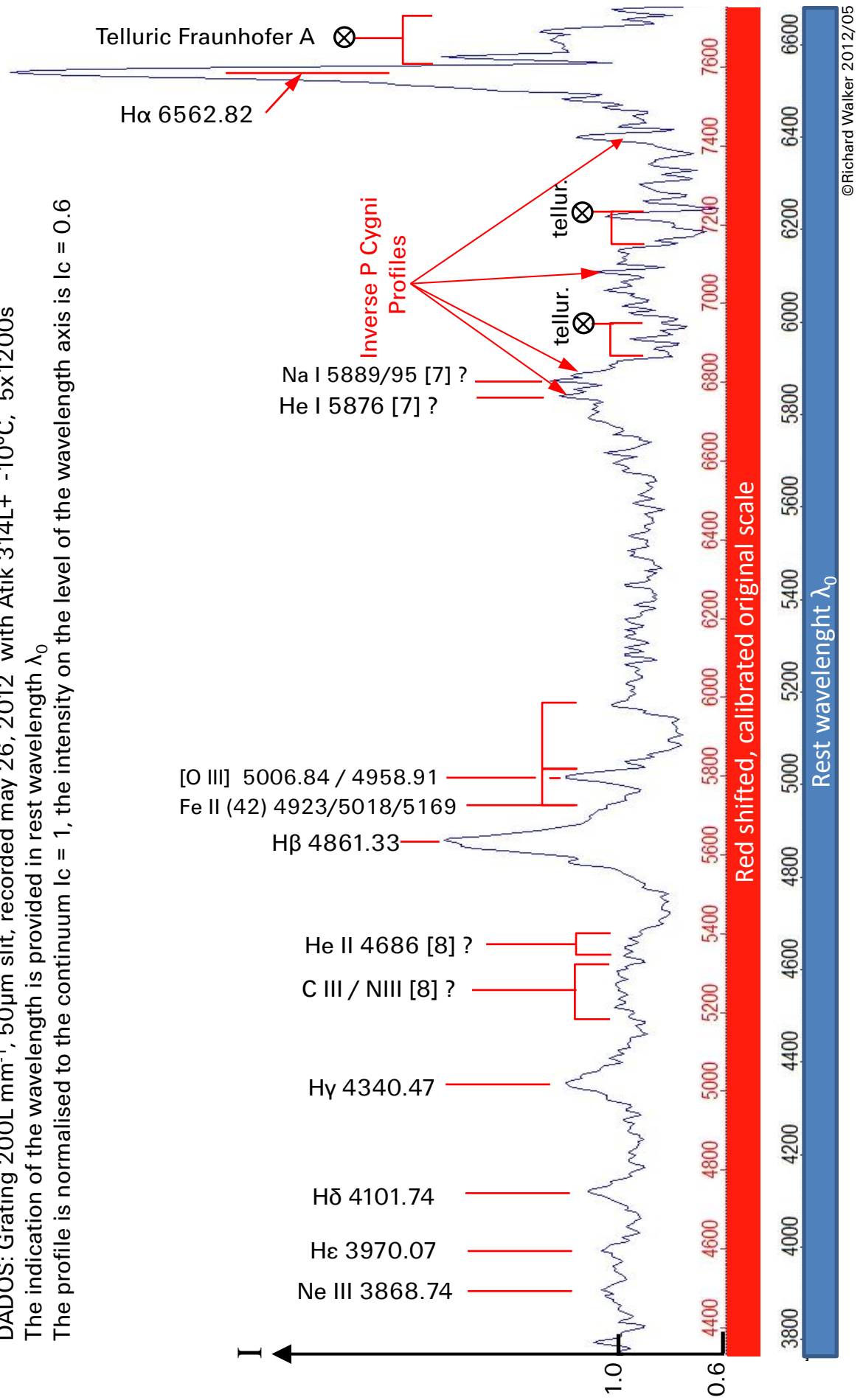
This is roughly within the strongly scattering literature values. To the question, in which areas around the Black Hole such velocities may occur, my searches have so far been unsuccessful. For the jet however, based on X-ray analyses, up to 70% of the speed of light are postulated [3].

# Quasar 3C273 Line Identification

DADOS: Grating 200L mm<sup>-1</sup>, 50μm slit, recorded may 26, 2012 with Atik 314L+ -10°C, 5x1200s

The indication of the wavelength is provided in rest wavelength  $\lambda_0$

The profile is normalised to the continuum  $I_c = 1$ , the intensity on the level of the wavelength axis is  $I_c = 0.6$



## 5 The Redshift of the Spectral Profile

Preliminary remark: In this section 5 and on the following table, redshifted wavelengths are indicated, measured at Gaussian fitted lines and related to the original wavelength scale, calibrated with a modified OSRAM glowstarter bulb [25]. The radial velocity  $v_r$  is calculated here with the Doppler formula.

$$v_r = \frac{\Delta\lambda}{\lambda_0} \cdot c \quad \{2\} \qquad \Delta\lambda = \frac{v_r \cdot \lambda_0}{c} \quad \{3\}$$

If formula {2} is converted for the explicit calculation of the Redshift  $\Delta\lambda$  {3}, we can recognise, that at a given radial velocity, the amount of the shift  $\Delta\lambda$  is proportional to the rest wavelength  $\lambda_0$  of the corresponding spectral line. This can impressively be seen in the spectrum of 3C273. While the H $\alpha$  line, with the rest wavelength of 6563Å, is shifted by the huge amount of about 1017Å to  $\lambda$  7580Å (!), the Redshift of the H $\delta$  line amounts here to just 646Å.

In the field of astrophysics for such highly red shifted objects, the distance is usually expressed directly as  $z$ -value. It can easily be determined by the measured Redshift in the spectrum and is independent of assumptions for cosmological model parameters (eg  $\Omega$ ). Due to the constant speed of light  $c$ ,  $z$  is also used as a measure of time for the past.

$$z = \frac{\Delta\lambda}{\lambda_0} \quad \{4\}$$

The dimensionless  $z$  - values remain independent from the wavelength of the analysed line. In the following table they are listed for all H-Balmer lines in the profile of 3C273, with the exception of the split H $\alpha$  emission. A heliocentric correction is not necessary here, because the apparent "recess velocity" reaches almost 20% of the speed of light!

Line	$\lambda_{redshifted} (*)$	$\lambda_0$	$\Delta\lambda$	$z$
H $\beta$	5632	4861	771	0.1586
H $\gamma$	5023	4340	683	0.1574
H $\delta$	4748	4102	646	0.1574

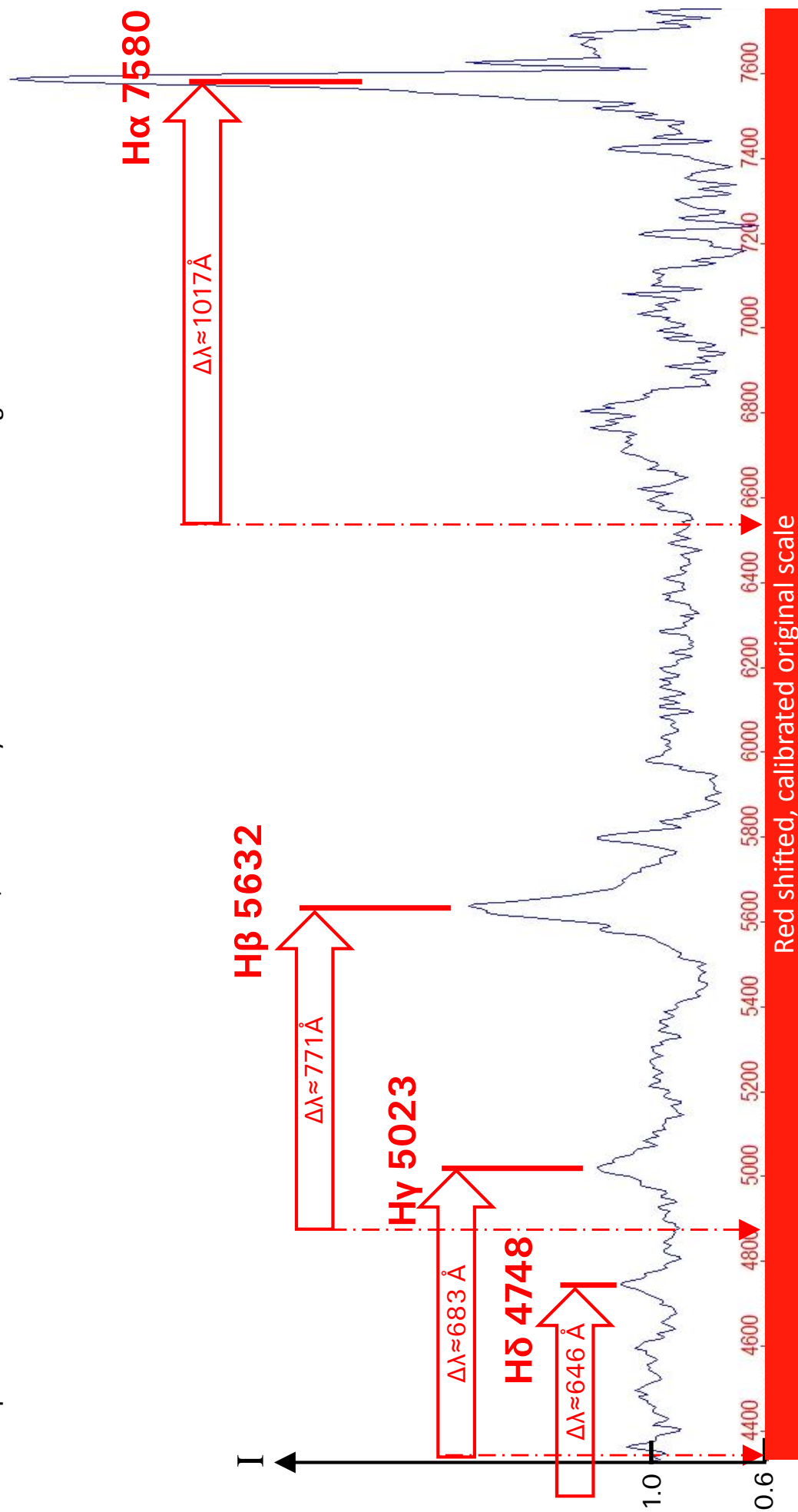
(\*) measured with Vspec at Gaussian fitted lines

According to [1] and [2] the accepted value is  $z \approx 0.1583$ . Thus the present measurements are consistent here up to almost three decimal places. There exist Quasars with Redshifts up to  $z > 7$ . Accordingly in the literature one can find spectral lines in the optical part of the profile, which under normal conditions are located in the UV region of the spectrum, such as L $\alpha$  of the Lyman series. Therefore, it becomes understandable why current and future space telescopes will be increasingly optimized for the infrared range of the spectrum.

# Quasar 3C273, Redshift of the Hydrogen Balmer Lines

DADOS: Grating 200L mm<sup>-1</sup>, 50μm slit, recorded may 26, 2012 with Atik 314L+ -10°C, 5x1200s

The indication of the wavelength, determined with Vspec at Gaussfits, is provided red shifted on the original scale  
The profile is normalised to the continuum  $I_c = 1$ , the intensity on the level of the wavelength axis is  $I_c = 0.6$ .





## 6 Estimation of the Apparent Recession Velocity

With the known  $z$  value we can estimate now the apparent recession velocity. "Apparent" means that the object is not cinematically moving away from us, but the space in between or the so-called "space-time lattice" is expanding [10]. Consensus seems to prevail here amongst the cosmologists.

$$v_f = c \cdot z \quad \{5\}$$

For 3C273 we get  $v_f \approx 47'490 \text{ km s}^{-1}$ . But it is easy to see that for values  $z > 1$  also  $v_f$  would be greater than the speed of light. Thus, the application of formula {5} is limited to  $z \ll 1$ , to avoid a violation of the Special Relativity Theory (SRT). For such extreme cases a simple, modified Doppler formula is available that takes into account the effects of SRT [9].

$$v_r = c \cdot \frac{(z + 1)^2 - 1}{(z + 1)^2 + 1} \quad \{6\}$$

With this formula the "recession velocity" of 3C273 is now significantly reduced to:

$$v_f \approx 43'808 \text{ km s}^{-1}$$

This is well consistent with  $43'751 \text{ km s}^{-1}$ , the according value in the CDS database [1].

## 7 Estimation of the Distance

The classical method to estimate the distance  $D$  is based here on the Hubble's law.

$$v_f \approx c \cdot z \approx H_{(t)} \cdot D \quad \{7\} \quad \text{Hubbleparameter } H_{(t)} \approx 73 \text{ km s}^{-1} \text{ Mpc}^{-1}$$

By converting of formula {7} we get the distance  $D$  in [Mpc]

$$D \approx \frac{c \cdot z}{H_{(t)}} \quad \{8\}$$

Formula {8} also expresses that the distance  $D$  increases proportional to the Redshift  $z$ . Thanks to advances in technology even amateur astronomers have nowadays the pleasure to deal with cosmologically relevant distance ranges. We must therefore be aware of the *effects* of the SRT as well as of the cosmological models, which are still under debate. That includes that the classical imagination of "distance" becomes increasingly unrealistic, and the Hubble's law, for  $z > 0.1$  ( $\sim 400 \text{ Mpc}$ ), may no longer be applied proportional, ie without consideration of cosmological model parameters [10]. The Redshift of 3C273 is already clearly above this "permitted" limit. So it is understandable that both, CDS [1] as well as NED/NASA [2] just provide the  $z$ -value. Nevertheless if we apply the Hubble's law conventionally, we obtain a distance  $D$  of about  $650 \text{ Mpc}$ , or  $2.12 \text{ bn light years}$ . The literature values are slightly higher in the range of some  $2.5 \text{ bn light years}$ .

In the world of the Messier Galaxies, the  $z$ -and  $v_f$  values are comparatively very modest. Record holder is M88 with  $z \approx 0.0076$  corresponding to  $v_f \approx 2281 \text{ km s}^{-1}$ .

## 8 Variations in the Spectral Profile

The table on page 11 shows a montage of two profiles. They have been recorded within only 12 days and are normalised on the same section to  $I_c = 1$ . In the first profile, recorded May 14, 2012, the H $\alpha$  line is missing, because by the initial setting of the wavelength range the expected massive Redshift has been simply forgotten. The hydrogen Balmer lines and the O III emission of the two profiles appear not significantly different. However, striking in the profile of May 14, 2012 is the highly elevated “bump” in the range of about 7000Å, which is still superposed by an emission of unknown origin. Another difference is noted in the area around 6100 Å.

The example shows impressively that significant variations can occur in this spectrum within a relatively small period of time. It also shows that this central region can't be indefinitely large, and according to [www.hubblesite.org](http://www.hubblesite.org) can therefore hardly exceed the diameter of our solar system. 3C273 would certainly be a highly interesting candidate for a monitoring project.

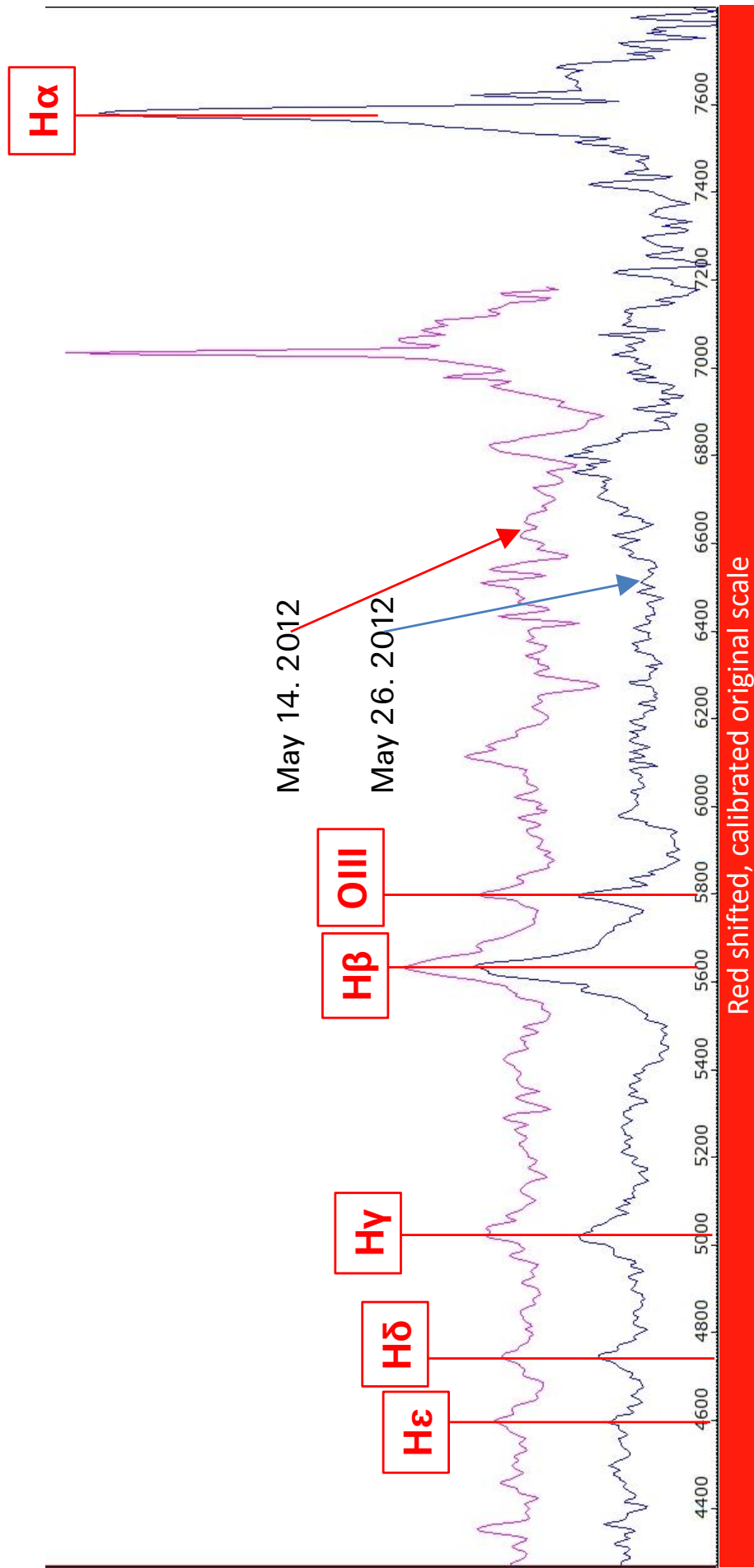
Important: In addition to such considerations we should always be aware that these changes, observed within a very short time, took place about 2.4 billion years ago, when our earth was still in the Precambrian geological age!

## 9 Relative Radiometric Flux Correction of the Profile

The table on page 12 is intended to provide a rough, qualitative impression of the relative flux of the Quasar continuum. The correction curve was generated here with the synthetic standard profile of an O5 type star in the Vspec Library, because Quasars radiate excessively in the UV and X-ray range. A comparison of 3C273 with the pseudo-continuum of a spectral type O 9.5 star, which was recorded with the same setup, shows a very similar course of the profiles. Thus, this procedure appears to be admissible even though it remains unclear to what extent the environment of a “Black Hole” matches to the radiation characteristics of a “Black Body”.

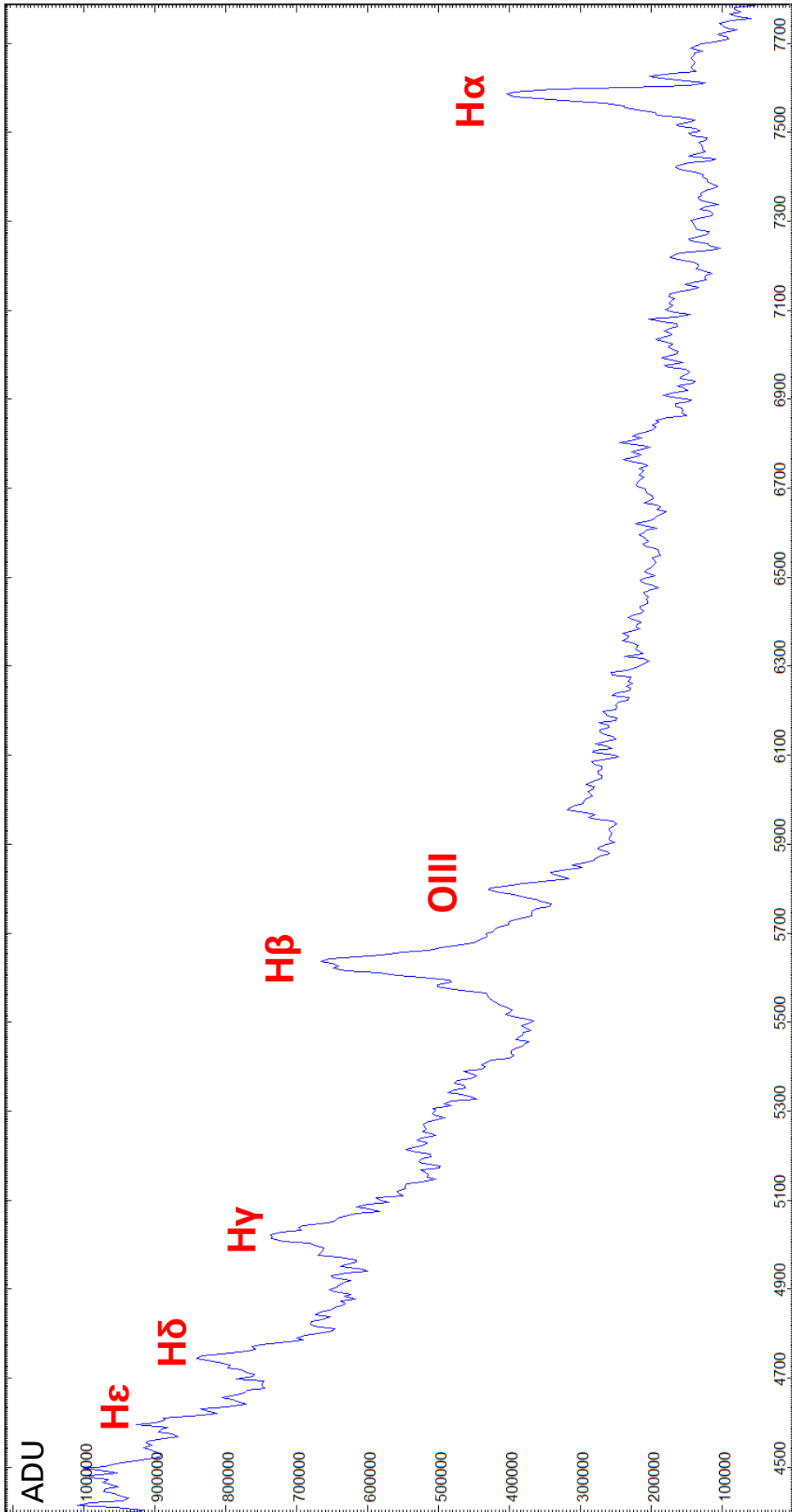
# Quasar 3C273 Variations in the Spectral Profile

DADOS: Grating 200L mm<sup>-1</sup>, 50μm slit, recorded may 14, and 26, 2012 with Atik 314L+ -10°C, 5x1200s  
The indication of the wavelength corresponds here to the original red shifted scale  
The superposed profiles are normalised to the continuum  $I_c = 1$  and shifted in parallel by an integer



# Quasar 3C273 Profile with Relative Radiometric Flux-Correction

DADOS: Grating 200L mm<sup>-1</sup>, 50μm slit, recorded may 26, 2012 with Atik 314L+ -10°C, 5x1200s  
The indication of the wavelength is provided red shifted on the original scale. The intensity scale shows ADU.  
The profile is relatively Flux-corrected, based on a correction curve, generated with a synthetic O5 Standard star (Vspec).



Red shifted, calibrated original scale

## 10 Recording of the Spectrum – Considerations and Details

Up to now such faint objects were generally regarded as the domain of the (slitless used) transmission grid. This is shown by numerous examples of 3C273 as well as of extragalactic Supernovae, recorded by amateurs. Christian Buil has recently shown with LISA [11], that it also works with a slit spectrograph with a much higher resolution and an unequally better calibration precision. The first signs that this could succeed with DADOS brought the record of the Protostars, *T Tauri* and *R Monocerotis* for the Spectroscopic Atlas [21]. It has now turned out that with  $V \approx 12.7^m$  3C273 probably represents not even the lowest brightness limit of this setup. Thus more Quasars, with a slightly lower brightness, move here in the realistic range. The Manual of 2008 estimated the limiting magnitude of DADOS to approximately  $8^m$ , based on 30 cm aperture, an exposure time of 20 minutes and  $9\mu\text{m}$  pixel size.

The quasi-stellar, pointlike appearance of the Quasar considerably facilitates the recording of the spectrum. The nebula of the very faint Supernova remnant M1 was much more difficult and required a minimum of 30 minutes per single shot. With the C8, the  $200\text{L mm}^{-1}$  grating and the Atik 314L+, cooled to  $-10^\circ\text{C}$  and applied in  $2\times 2$  binning mode, 20 minutes exposure time have been sufficient. The result is a somewhat noisy profile which would already allow a rough determination of the Redshift. The addition of five such profiles already reveals fine structures and allows the determination of the Redshift with an accuracy of nearly three decimal places. For a high quality astrophotography, much more exposure time must be applied!

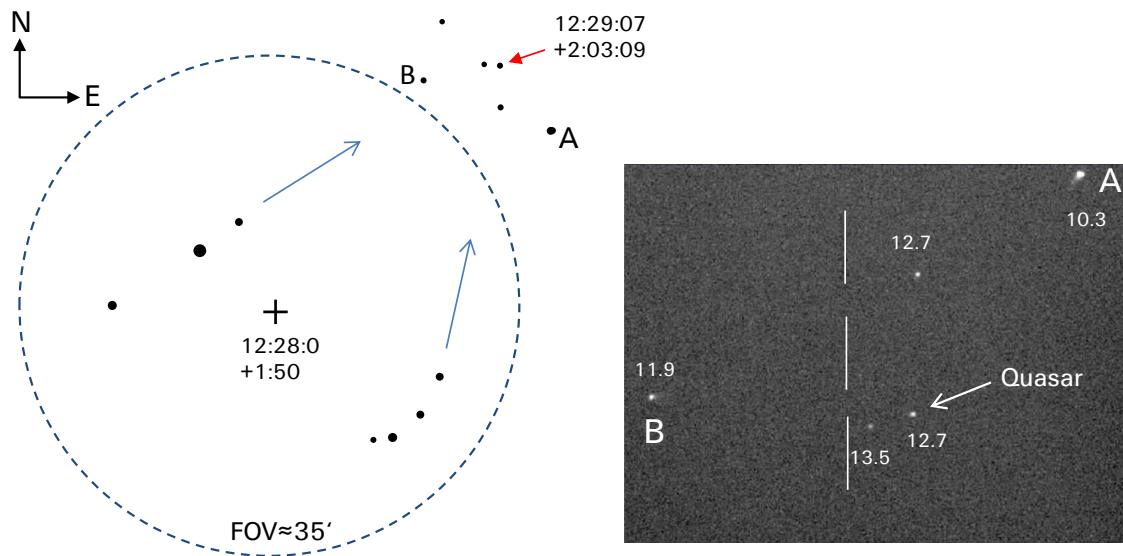
Due to the small pixel size of  $6.45\mu\text{m}$ , the application of the  $2\times 2$  binning mode barely impairs here the resolution, even not with the smallest  $25\mu\text{m}$  slit. However the required exposure time is considerably more than halved thereby. At fainter objects, applying the  $50\mu\text{m}$  slit, even the  $3\times 3$  binning mode could be used with a little loss of resolution.

With such long exposure times in our densely populated areas, the light pollution artefacts must be subtracted from the recorded spectrum (see [21] sect. 27). In Vspec, for point light sources and long slits this can directly be done together with the sky background, based on the same spectral image.

The PHD autoguiding was performed with the DSI II slit camera on a neighbouring faint star. The C8 is mounted on a Vixen Sphinx SXD Deluxe. An exposure time of 3.5s has been applied. Anyway a very clear sky is required without any thin cirrus clouds.

To facilitate the orientation, finally a finding chart is attached. The blue circle on the left shows the field of view (FOV) in a 25mm eyepiece at about 2000mm focal length (C8), on a flip mirror, mounted between telescope and spectrograph. Within the circle two distinct star rows can be seen. They serve here as "pointer stars" to the faint star group, which hosts 3C273. Star **A** is there by far the brightest with  $10.3^m$ .

The indicated magnitudes are based on AAVSO enabling a rough estimation of the "current" luminosity of 3C273. The object of course can also be approached directly on its coordinates. The screenshot at right shows the apparent Quasar environment on the PHD Guiding screen, taken with my DSI II slit camera. The star, directly adjacent to 3C273, is slightly weaker with some  $13.5^m$ .



## 11 Bibliography and Internet Links

### Database:

[1] CDS Strassbourg: *SIMBAD Astronomical Database*  
<http://simbad.u-strasbg.fr/simbad/>

[2] NASA Extragalactic Database (NED)  
<http://nedwww.ipac.caltech.edu/>

### Literature and Links:

[3] M. J. Avara, *Precision X-Ray Spectroscopy of 3C273 Jet Knots*, MIT 2008  
<http://dspace.mit.edu/bitstream/handle/1721.1/44464/297176629.pdf?sequence=1>

[4] B.M. Peterson et al. *Are Forbidden Lines Present in the Optical Spectrum of the QSO 3C 273?* Ohio State University 1984 <http://articles.adsabs.harvard.edu/full/1984ApJ...283..529P>

[5] B.M. Peterson et al. *Central Masses and Broad-Line Region Sizes of Active Galactic Nuclei. II. A Homogeneous Analysis of a Large Reverberation-Mapping Database*. The Astrophysical Journal 2004 <http://arxiv.org/abs/astro-ph/0407299>

[6] S. Paltani, M. Türlér: *The mass of the black hole in 3C273*, 2005 Marseille, Geneva  
<http://arxiv.org/abs/astro-ph/0502296>

[7] A. Boksenberg et al. *New Spectrometric Results on the Quasar 3C273*, University London 1974  
<http://adsabs.harvard.edu/full/1975MNRAS.172..289B>

[8] J.B. Oke: *The Optical Spectrum of 3C273*, CALTECH 1964  
<http://adsabs.harvard.edu/abs/1965ApJ...141....60>

[9] Fritz Kurt Kneubühl, *Repetitorium der Physik*, Teubner Studienbücher Physik, Kap. *Relativistischer Doppler-Effekt der elektromagnetischen Wellen*

[10] Lexikon Astronomie Wissen, Andreas Müller, TU München  
<http://www.wissenschaft-online.de/astrowissen/>

[11] Christian Buil: *Observations avec le Spectrographe Lisa*  
<http://www.astrosurf.com/buil/lisa6/obs.htm>

### Author:

The following scripts on the subject (some of them in german) are downloadable under this link:  
<http://www.ursusmajor.ch/astrospektroskopie/richard-walkers-page/index.html>

[20] *Analysis and Interpretation of Astronomical Spectra, Theoretical Background and Practical Applications for Amateur Astronomers*

[21] *Spectroscopic Atlas for Amateur Astronomers, A Guide to the Stellar Spectral Classes*

[22] *Das Aufbereiten und Auswerten von Spektralprofilen mit den wichtigsten IRIS und Vspec Funktionen*. Unter dieser Homepage ist alternativ ein Tutorial von Urs Flükiger zu finden, mit Hauptgewicht auf der Bildbearbeitung.

[23] *Kalibrierung von Spektren mit der Xenon Stroboskoplampe*

[24] *Atomic Emission Spectroscopy with Spark- or Arc Excitation, Experiments with the DADOS Spectrograph and Simple Makeshift Tools*

[25] *Kalibrierung von Spektren mit dem Glimmstarter ST 111 von OSRAM*

[26] *Glow Starter RELCO SC480, Atlas of Emission Lines*